Can active perception generate bistability?

Heterogeneous collective dynamics and vascular patterning

Katie Bentley[1], Kyle I Harrington [2] and Erzsébet Ravasz Regan[1]

[1]Beth Israel Deaconess Medical Center, Harvard Medical School, Boston MA
[2]DEMO Lab, Computer Science Department, Brandeis University, Waltham, MA
kbentley@bidmc.harvard.edu

Abstract

During morphogenesis (the generation of form), biological cells, agents or robots must collectively coordinate where and when to move. How to solve such complex, spatial problems in a timely manner, is fundamental to survival in biological organisms, though temporal regulators are largely unexplored. We take the generation of new blood vessel networks (angiogenesis) as our case study system, where tissues low in oxygen stimulate endothelial cells "ECs" (the inner lining of blood vessels) to grow new network branches. This requires ECs to take on heterogeneous states by collectively competing with one another for migratory status via lateral inhibition.

We propose here that the traditional "decide then move" perspective of cell behavior in angiogenesis may miss a key temporal regulator as it is too slow to account for the rapid, adaptive assignment of heterogeneous cell states. Here we show that a "move and decide" view may provide a better account. In a study focused on an individual EC in a simulated collective, we find that active perception (sensorimotor feedback) can generate bistability through migration-induced cell shape changes. We further exemplify that when parameters affecting active perception are modulated, bistability is lost in the single cell. As a consequence, active perception can directly modulate collective decision timing.

Introduction

Collective behavior during morphogenesis requires timely coordination of many autonomous agents, which becomes increasingly complex if the task requires agents have heterogeneous and adaptive phenotypes. Understanding collective coordination mechanisms holds great promise for morphogenetic engineering of well-adapted robot designs (Doursat et al 2012). To this end, the vasculature in living systems is a perfect case study. New vessels grow and remodel in a dynamic adaptive way to maintain a network with near-intimate contact to every cell in the body, required due to the diffusion limit of Oxygen (Aird 2005). When new vessel growth (angiogenesis) is needed, e.g., in development or wound healing, endothelial cells (ECs) lining blood vessel tubes adaptively respond to the release of diffusing growth factors from hypoxic (low in oxygen) tissue. The ECs then collectively coordinate such that some cells migrate and lead new tubular branches ("sprouts"), while others line the tube walls and ensure that the branches are well spaced (Geudens and Gerhardt 2011) (Fig. 1a). The selection of these two states - "active" or "inhibited" cell movement - is known to be coordinated by Notch-driven "lateral inhibition", where cells battle to inhibit their neighbors (Hellström et al 2007, Jakobsson et al 2009). Lateral inhibition is known to generate stable alternating patterns of on and off cell states in many systems, hereafter referred to as a Salt and Pepper pattern "S&P pattern" (Collier et al 1996). Recently we showed, via an integrated *in silico* and *in vivo* approach, that cell states are not fixed once selected, but rather dynamically adapt and flip throughout angiogenesis (Bentley et al 2009; Jakobsson et al 2010; Bentley et al 2014a). This occurs when ECs 1) meet new neighbors during branch fusion (required to form

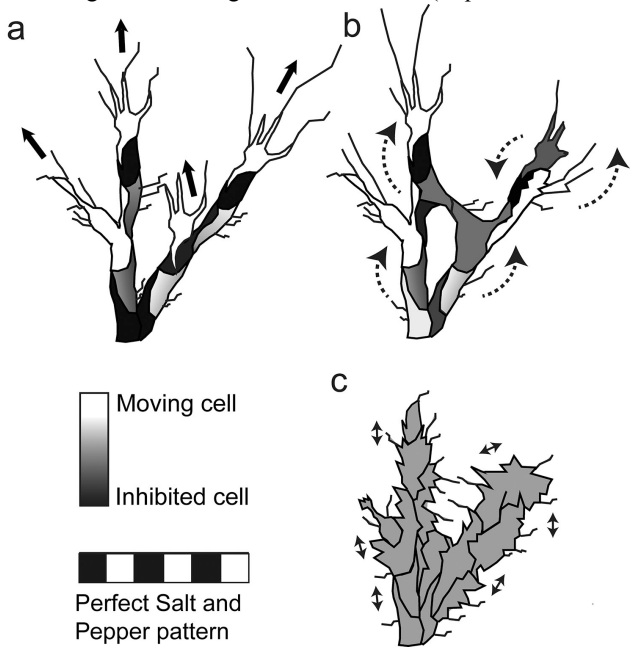

Figure 1. a) Endothelial cells, initially all the same, collectively coordinate to become heterogeneous when stimulated to grow new blood vessel branches. Some cells move, leading new sprouts, others are inhibited, lining the branch and keeping them regularly spaced. The optimal spatial arrangement is a "salt and pepper" (S&P) pattern (alternating states). b) During branching the branches fuse to forming new loops of the network and cells interchange positions. c) If reassignment of states is not rapid the system will fall into homogenous phases as the states are still deciding, disrupting well spaced branching and thickening vessels.

network loops and support blood flow; Fig 1b) (Bentley et al 2009) and 2) rearrange their positions in the collective (Jakobsson et al 2010). Thus, the cellular collective must be capable of rapidly re-establishing the S&P pattern of behaviors in the face of local neighborhood changes, to keep the network branching structure optimized. Otherwise, cells would drift into a "half-way house" state of homogenous movement (Fig. 1c). Lack of differential movement has been shown to disrupt branching as cells hypersprout instead (Hellstrom et al 2008), and has been implicated in abnormal vessel thickening in disease (Bentley et al 2014a). Here we ask, is there an extra dimension of temporal regulation that keeps the system from lingering in a homogeneous state as the process unfolds.

Do cells "Decide then Move" or "Move and decide"?

In Biology, signaling cascades regulating cell behavior are usually presented in a feed-forward manner (Fig. 2a). E.g. ECs are selected as migratory collectively, by Notch lateral inhibition and then those selected will migrate, they "*decide then move"*. However, the relative timing of events indicates that things may, in fact, be more complex.

Lateral inhibition communication between the ECs can be summarized as follows: each cell detects a diffusing stimulatory signal from the hypoxic tissue, primarily Vascular Endothelial Growth Factor (hereafter input signal,"*I*") by activation of its VEGFR receptors (hereafter sensors, "*S*"). Sensor activation leads to the up-regulation of the ligand Dll4 ("*D*"), which then binds to and activates Notch receptors ("*N*") on neighboring cells. When *N* is active, the cell down-regulates *S*. Several amplification cycles of this pathway then leads to one cell inhibiting the other's *ability to sense,* more than the inhibition it, itself, receives (see Figs. 2c-e).

The same sensors also trigger the migratory response of the cell, by locally activating the actin cytoskeleton to first polymerize, generating long thin membrane protrusions called "filopodia" that reach into the environment. Second, acto-myosin contractions and adhesion dynamics propel the cell forward. Thus a cell that is more inhibited by Notch signaling, will have less sensors and so will be less migratory (the "inhibited" state).

Lateral inhibition requires gene regulatory changes in the nucleus and protein synthesis, which can take on the order of hours. While faster than multiple cycles required for lateral inhibition, a full migratory response (e.g., where single cells rearrange their positions) also occurs on the time-scale of hours (Jakobsson et al 2010). However, the *initial* migratory response of filopodia growth occurs more rapidly (on the order of minutes) and locally (at the cell surface), without the need to alter gene expression. It is thus logical to assume that the cell shape changes (filopodia) and early movements of the cells membrane during the initial stages of migration will proceed ahead of the established collective decision making process of lateral inhibition.

Consequently, we propose a "*move and decide*" strategy better captures the process.It is important to note that, *the sensors themselves move rapidly during motion*, as they reside on the deforming membrane surface. As filopodia extend and retract, sensors are moved to new locations in the environment, continually changing their input (Fig 2c). If the environment contains a gradient, this process has been indicated to speed up collective decision making (Bentley et al 2008). However, the exact reason for this has not been

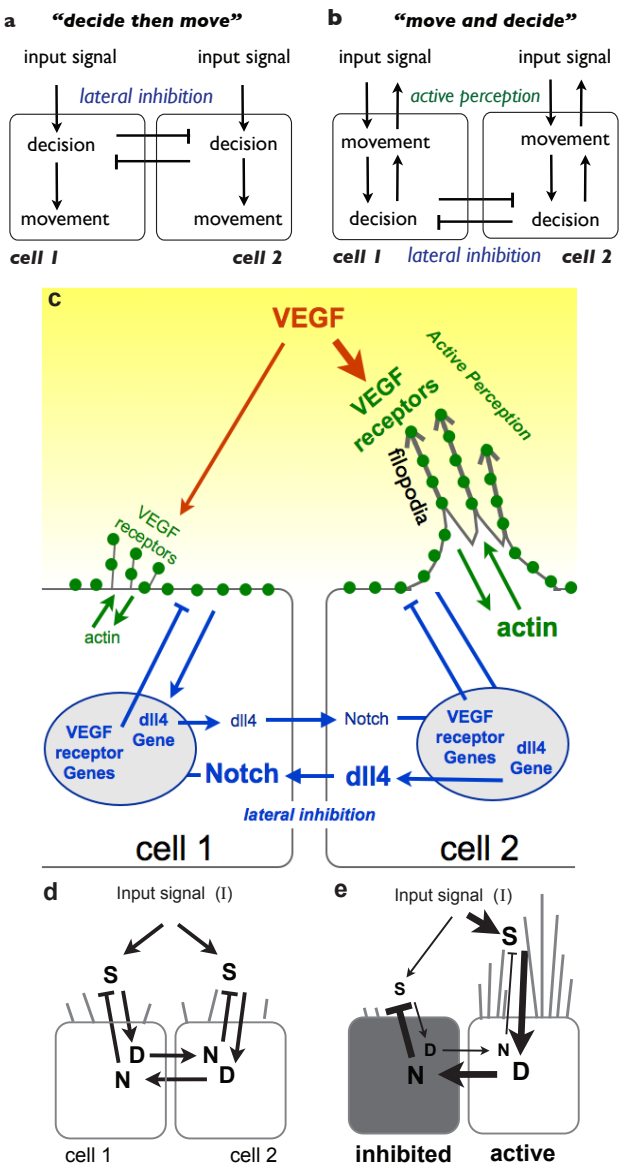

Figure 2. a) traditional feed-forward view of cell behavior regulation in biology termed here a "decide then move" strategy. b) The alternative "move and decide" strategy. c) Signaling pathways involved in blood vessel selection of heterogeneous movement behaviors. Green dots indicate that sensors (VEGFR receptors) reside on the cell membrane, which is deformed and moved as actin polymerizes to form filopodia creating a sensorimotor loop (active perception) d-e) simplified model of (c) *S* = sensors, *D* = Dll4, *N* = Notch, *I* = input signal. Overtime cells battle back and forth to inhibit each other with one eventually acquiring more filopodia and inhibiting its neighbor more.

established. Here we propose that filopodia act as a means to perform *active perception* of the tissue environment, similar to the proposition that flagella motion confer sensorimotor dynamics and indeed minimal cognition to migrating E. coli cells (Van Duijn et al 2006). While the importance of embodiment in vascular morphogenesis has recently been highlighted (Bentley et. al., 2014b), here we further posit that such active perception confers *bistability* to the active/

inhibited states, rather than the other way around, as currently thought.

An ability to continually adapt and inform our decision making as we move through and experience more of our environment via active perception is known to confer an advantage to decision making, with many studies in robotics and child development e.g. Piaget (1967), Pfeifer (1997) and Beer (2000). As Dewey (1896, pp.137-138) so elegantly put:

> *We begin not with a sensory stimulus, but with a sensorimotor co-ordination… In a certain sense it is the movement, which is primary, and the sensation which is secondary…"*

To establish whether active perception feedback by individual ECs in a "move and decide" strategy may confer robustness and optimize timing of collective decisions, we consider first a tightly controlled, single EC scenario, where collective coordination by lateral inhibition is de-coupled. We hypothesize that active perception alone, *prior* to any engagement of lateral inhibition feedback, can generate bistability of active/inhibited states. This crucially implies that in situations where single ECs experience intermediate levels of inhibition from their neighbors (common during collective decision making), bistability allows them to pre-commit to an activated or inhibited state. The subsequent lateral inhibition process is thus never called to amplify rapid random fluctuations in D difference between two neighbors. Rather, in each moment each single cell makes a clear decision, and presents its "vote" for lateral inhibition to amplify and lock in, speeding up coordinated decisions.

Bistability, hysteresis and positive feedback

The ability to dynamically select between two *distinct* phenotypes, while intermediate states are unstable, is a hallmark of bistable regulatory systems. In general, bistable systems can maintain two distinct locally stable states in a *single* environment. A simple mechanical analogy is that of a ball found on a double-well landscape (Fig. 3a). In this case, the physical shape of the landscape supporting the ball against gravity creates two stable states, i.e., the bottom of each well.

In the presence of any noise able to overcome friction between ball and surface, this mechanical system will not linger in an intermediate state, at the top of the barrier or between valleys. Positing an iron ball and an external magnet, it is also easy to appreciate that under certain environmental conditions (e.g. magnet on the right side of double-well) this system may be rendered mono-stable. Transitions between the two locally stable states take place abruptly, whenever forces on the ball exceed the potential barrier imposed by the presence of gravity. Moreover, slowly tuning the environment by moving the magnet position left to right and back again (such that the ball is restricted to the left / right / left valleys) uncovers a signature behavior of bistable systems, namely *hysteresis* (Fig. 3b). Charting the position of the ball as a function of the position of the magnet clearly reveals the initial-condition dependence of the ball's response. For any position of the magnet within a window around the barrier, the ball can settle into either of the two valleys, but which one depends on its recent history of positions. It cannot be stable in the transition state on top of the barrier, it will fall into one

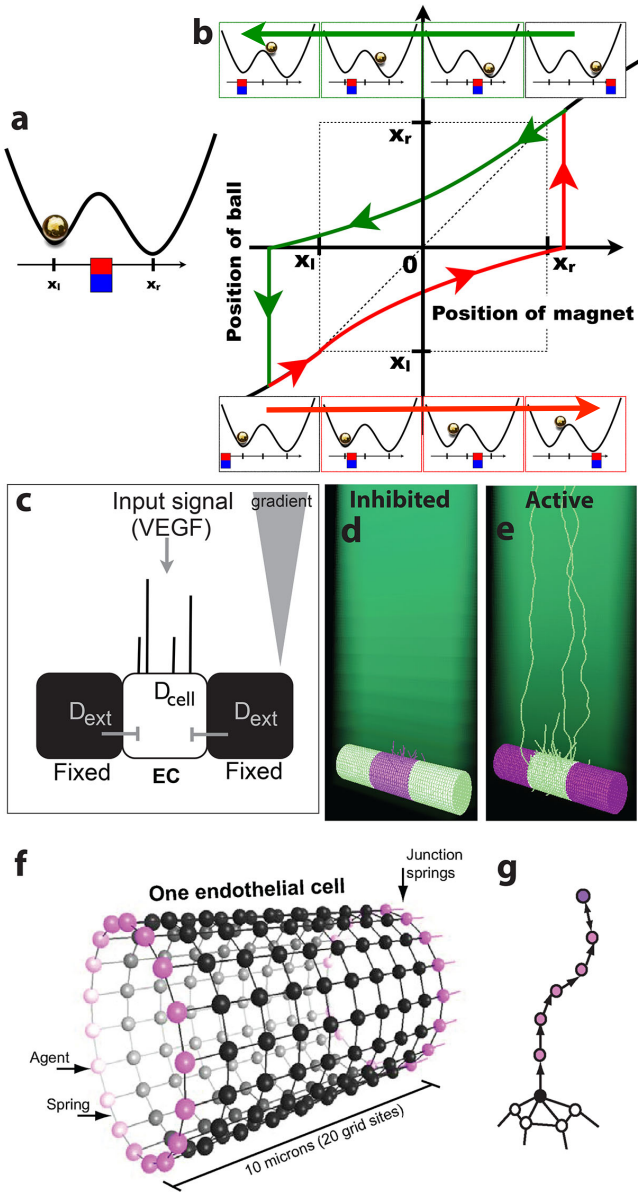

Figure 3. a) A mechanical bistable system - metal ball in a gravitational double-well potential. b) Moving a strong magnet under the ball acts as environmental input, capable of restricting the ball into a single well. As the magnet is slowly shifted from left to right (x-axis), the ball's position (y-axis) first changes slowly (bottom row; red), then undergoes an abrupt jump as the ball clears the barrier. Reverse arm: top row, green. In a wide region of magnet-positions, the ball's dynamics are bistable: it can reside in either valley depending on its initial conditions. c) The APB model setup, we track a single EC's activity (D_{cell}) as it responds to I in the environment and D_{ext} from its fixed neighbor cells. d-e) Frames at t = 300 from APB simulations, D levels high to low shown light green to purple, I gradient in environment shown dark green. d) A run where fixed neighbors have D_{ext} = 10000 (D_{max}) the central EC becomes inhibited (few short filopodia and low D_{cell}). e) A run where D_{ext} = 0, the EC becomes active, D_{cell} is high and it has lots of long filopodia. f) The memAgent Model of an EC, reproduced from (Bentley et al 2009). The cell membrane is represented by a

cylindrical, single layer square lattice mesh of agents "memAgents", connected by springs. At either end (adjacent cells not shown) specialized junction springs and agents (pink) connect the cell to its neighbor cells along the vessel. g) To grow a filopodium new memAgents and springs are created.

of the valleys.

How can active perception endow ECs with such bistability? In regulatory circuits, bistability usually arises due to positive feedback (Angeli et.al., 2004; Cherry and Adler, 2000; Gardner et al., 2000; Ferrell, 2002). Active perception through filopodia and cell shape changes that extend the sensors to areas with high levels of input signal generate a potent regulatory drive for further filopodia extension (Fig. 2c). We therefore hypothesize that at intermediate levels of lateral inhibition by neighbors (when collective decisions are still in process) filopodia extensions are difficult enough to initiate that an inhibited state is locally stable. At the same time, should the cell already possess a large number of filopodia extended into a steep input gradient, these send enough signal back to stabilize and maintain an active moving state (Fig. 3g).

The Active Perception Bistability (APB) Model

To test our hypothesis, we developed a new simulation testbed that parallels the above mechanical example. We focus on how an individual cell's state changes as it experiences different, controlled levels of inhibition from two immobilized neighbor cells. Lateral inhibition from these two neighbors ("External D" or D_{ext}) affects the individual EC under investigation (its current D level, "D_{cell}", is used as proxy for its active/inhibited state), but these neighbors are uncoupled from being inhibited themselves (Fig 3c). D_{cell} is therefore analogous to the "ball" in the mechanical example of a bistable system and the fixed neighbors to the magnet; raising D_{ext} can push the cell into a more inhibited (low D_{cell}) state and vice versa (Fig. 3d,e).

To simulate this scenario we use the memAgent Spring model (MSM model), which has been previously calibrated to experimental angiogenesis data – for full methods see Bentley et al (2008, 2009). Briefly, in this model cell morphology is represented as a surface comprised of many small agents (membrane agents, "memAgents") connected by springs following Hooke's law (which confer tension to the changing cell shape, akin to the actin cortex beneath a cells membrane) (Fig. 3f). The cell is 10 microns wide with 6 microns diameter (matching in vivo capillary dimensions). The world around it has dimensions (x,y,z = 30,58,10 microns). The memAgents move in continuous space, but are snapped to a gridded lattice to implement local rules (grid sites represent 0.5x0.5x0.5 micron cubes of space).

At each time-step an equal number of the cell's current, total sensors (S_{cell}) are distributed equally to each memAgent (S_m) over the cell's current surface shape. Dll4 ligands (D) are equally distributed to any memAgent in Moore neighborhoods of memAgents from other cells (on the interface between cells or "junctions"). The input signal (I) is modeled as a fixed linear gradient, where each grid site G above the vessel has I_G level, calculated as $I_G = V \cdot y$ where y is the y axis coordinate position of G and V is a tunable constant.

Signaling: Simplifying the description of the competitive receptor biology between different VEGFRs in the original MSM model, as it is not the direct focus of this study, we can state that the number of active sensors of a given memAgent m is calculated as $S'_m = S \cdot \sum I_G$. Notch is activated in each memAgent (resulting in the local removal of D from neighboring cell's memAgents), up to the value of N_m. If $D < N$ then $N'_m = D$; if $D > N$, then $N' = N_{max}$.

Filopodia: memAgents extend filopodia by one grid site length at a time by creating non-branched chains of new memAgents adhered to the environment (fixed position) (Fig. 3g). These events are stochastic, with probability:

$$P(\text{extend filopodia}) = F \cdot S',$$

where F is a tunable constant. For full rules behind the actin dynamics, springs and enforcing the chain extension see Bentley et al (2009). Filopodia retract if the memAgent at the top of the chain has not extended for 10 time steps, which is more likely when sensors do not activate. They retract by iteratively snapping the chain of springs back to the next memAgent in the chain, whilst deleting memAgents as they go (based on *in vitro* observations). The cells have no limit on the length of a single filopodium, or how many they can initiate. However, their total length cannot exceed the total amount of actin available to the cell. The original model in Bentley et al (2009) generates full cell migration by releasing filopodia adhesions and allowing the springs to pull the cell forward. Here, however we keep adhesions fixed to control variables and ask whether shape changes due to filopodia alone can generate bistability.

Genetic Regulation: Briefly, the lateral inhibition is implemented each time step as follows:

$$S_{cell} = S_{max} - \sigma N''_{cell}$$

$$D_{cell} = D_{cell} + \delta S''_{cell}$$

where σ, δ are constants and S'' denotes S' after a time delay (28 time steps) corresponding to the time it takes for transcription to alter gene expression in the nucleus, and subsequently protein levels at the cell surface. The new S_{cell} and D_{cell} levels are then redistributed to the memAgents and the process repeats on the next timestep.

Parameterization: All parameters in the model are set as in Bentley et al (2009), which were previously calibrated to experimental data. To investigate active perception we focus here on simulations varying its critical determinants: filopodia extension (F) and the input signal gradient (V). For normal EC behavior $F = 2$ and $V = 0.04$.

Results

Hysteresis simulations

We start with D_{ext} set to zero and thus simulate a fully active EC with long filopodia (Fig. 3e). We then slowly raise

the D_{ext} in increments of 50 until full inhibition is achieved, then reverse the process until it is yet again relieved. If active perception indeed creates bistability, we expect the transition between active/inhibited states to take place abruptly, at a D_{ext} threshold that is higher for the active → inhibited transition than the reverse. In order to approximate quasi-static equilibrium while changing D_{ext}, we tested the stability of D_{cell} levels using the following method: 1) we allowed a transient time window (250 time-steps) to pass, 2) we calculated the average and standard deviation of D_{cell} in two adjacent, non-overlapping sliding windows of size 250, 3) we tested whether $|\mu_c - \mu_p|/(\mu_c + \mu_p) < \varepsilon$ and $|\sigma_c - \sigma_p|/(\sigma_c + \sigma_p) < \varepsilon$, where μ_c/μ_p denote the average D_{cell} and σ_c/σ_p its standard deviation in the last/previous window ($\varepsilon = 0.5$). If the EC does not pass the

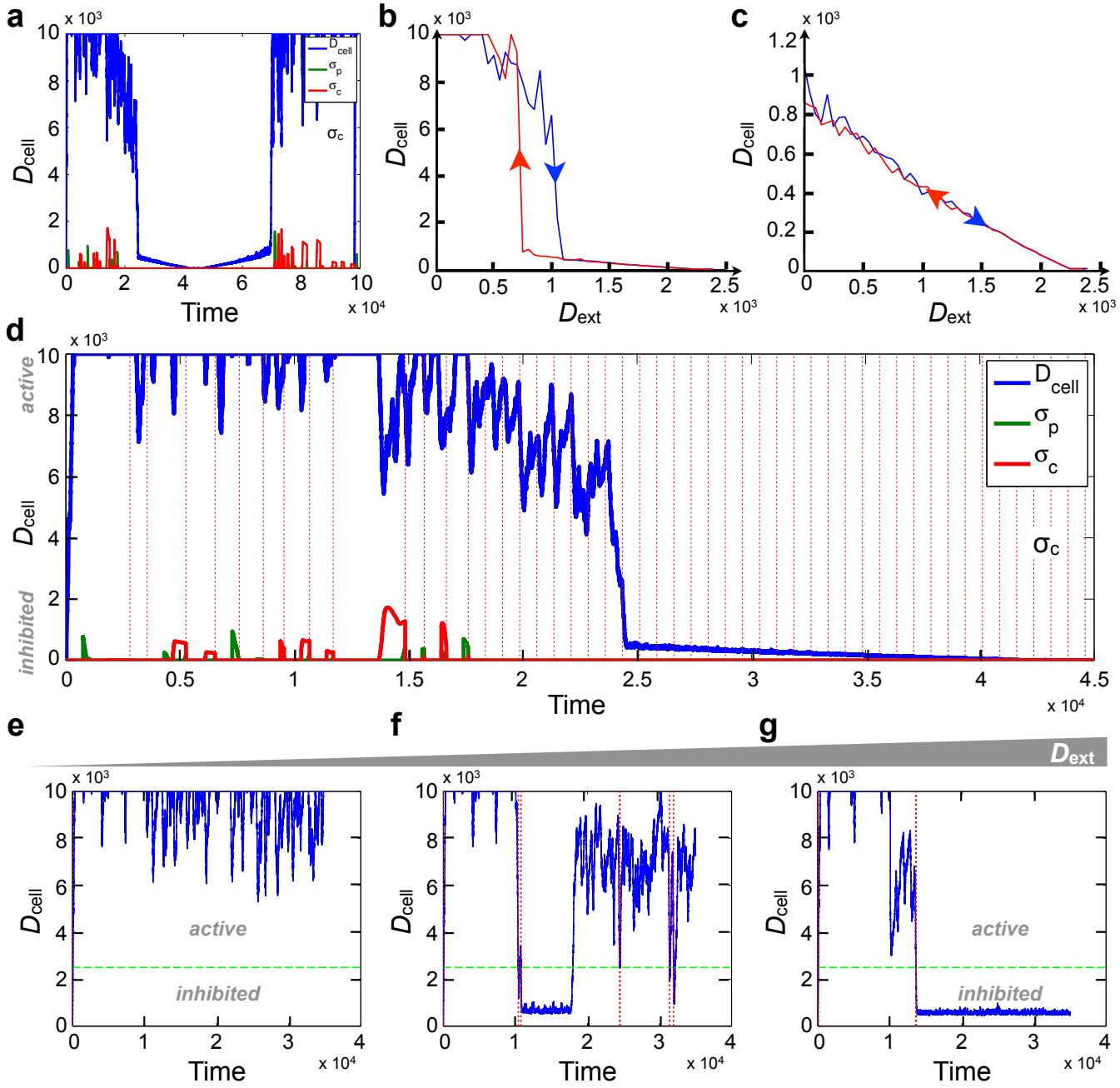

Figure 4. a) Time course of D_{cell} during a full cycle of hysteresis (blue). Standard deviation of D_{cell}, measured in two non-overlapping, expanding windows (σ_p for previous and σ_c for current windows) are shown in green and red, respectively. b) Hysteresis in the active / inhibited transitions of a single EC exposed to slowly increasing (blue), then decreasing (red) D_{ext}. c) Loss of hysteresis in a single EC with weak filipodia extensions, due to reduced sensorimotor feedback. d) Zoomed-in time course of D_{cell} during a half-cycle of hysteresis, showing large D_{cell} fluctuations in the active state. Red lines: times of D_{ext} increment. e-g) Long D_{cell} time-courses of ECs exposed to fixed D_{ext}. Green line: rarest observed D_{cell} value, marking the position of the barrier. Red line: transitions between active/inhibited states. e) $D_{ext} = 500$; EC restricted to the active state. f) $D_{ext} = 850$; bistable EC stochastically transitioning between active and inhibited states. g) $D_{ext} = 950$; EC restricted to its inhibited state.

test or a maximum time limit 60,000 was not yet reached, we increment the window. Otherwise we move on to the next D_{ext}. Figure 4a shows the time-dependent evolution of D_{cell} through a full hysteresis cycle, along with its standard deviation measured in each window. As Figure 4b indicates, the system shows hysteresis behavior: as D_{ext} increases (blue arm of hysteresis curve), the cell goes through an abrupt transition from active (high D_{cell}) to an inhibited state. Slowly decreasing D_{ext} (red arm) also leads to an abrupt transition from inhibited to active state, but D_{ext} needs to be lowered below the point at which the initial inhibition occurred. This indicates that there is a region of D_{ext} where the EC can exist in either its active or inhibited state, depending on its history.

To prove that active perception is required for this bistability, we repeated the simulations decreasing the rate of filopodia extensions (F) to half their normal value. When the filopodia-dependent sensorimotor feedback is thus weakened, the EC looses its bistability and becomes tunable, in that D_{cell} decreases proportionally with D_{ext} (Fig. 4c).

Due to the stochastic nature of filopodia extensions, D_{cell} fluctuations close to the bistable region are large (Fig. 4d; this is the rationale for the generous ε threshold of 0.5). Due to this inherent stochasticity, the exact D_{ext} thresholds at which abrupt transitions occur are not the same from simulation to simulation. Moreover, if the time window between increments is very large (well above the biological time scales involved in patterning), the EC may undergo stochastic transitions between metastable active/inhibited states. To understand the nature of these transitions, we set up a second set of simulations. In this case, we started the EC with $D_{ext} = 0$ and ran the simulation for 10^4 time steps, after which we abruptly increased D_{ext} to a nonzero target value, and performed $3 \cdot 10^4$ more steps. Figure 4e indicates that exposure to low D_{ext} (500) keeps the EC in an active state, albeit with sizable D_{cell} fluctuations. At the intermediate D_{ext} level of 850, however, the long simulation showcases abrupt, stochastic transitions between active and inhibited states (Fig. 4f). Lastly, high D_{ext} (950) causes a one-way transition from active to a strongly inhibited state (Fig. 4g). Even here, the transition is not immediate (~$0.3 \cdot 10^4$ steps), but it is irreversible within the time window of the run.

To understand the dependence of the ECs residence time in each state, we partitioned D_{cell} values into active and inhibited

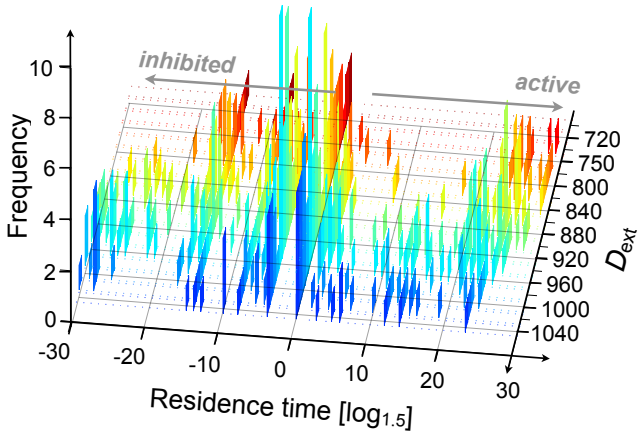

Figure 5. Distribution of residence times in the active and inhibited state (indicated by positive and negative x-values, respectively) in the course of long simulations in the presence of constant D_{ext} (red:low to blue: high). As D_{ext} increases, long residence times in the inhibited state gradually appear, while residence in the active state shortens.

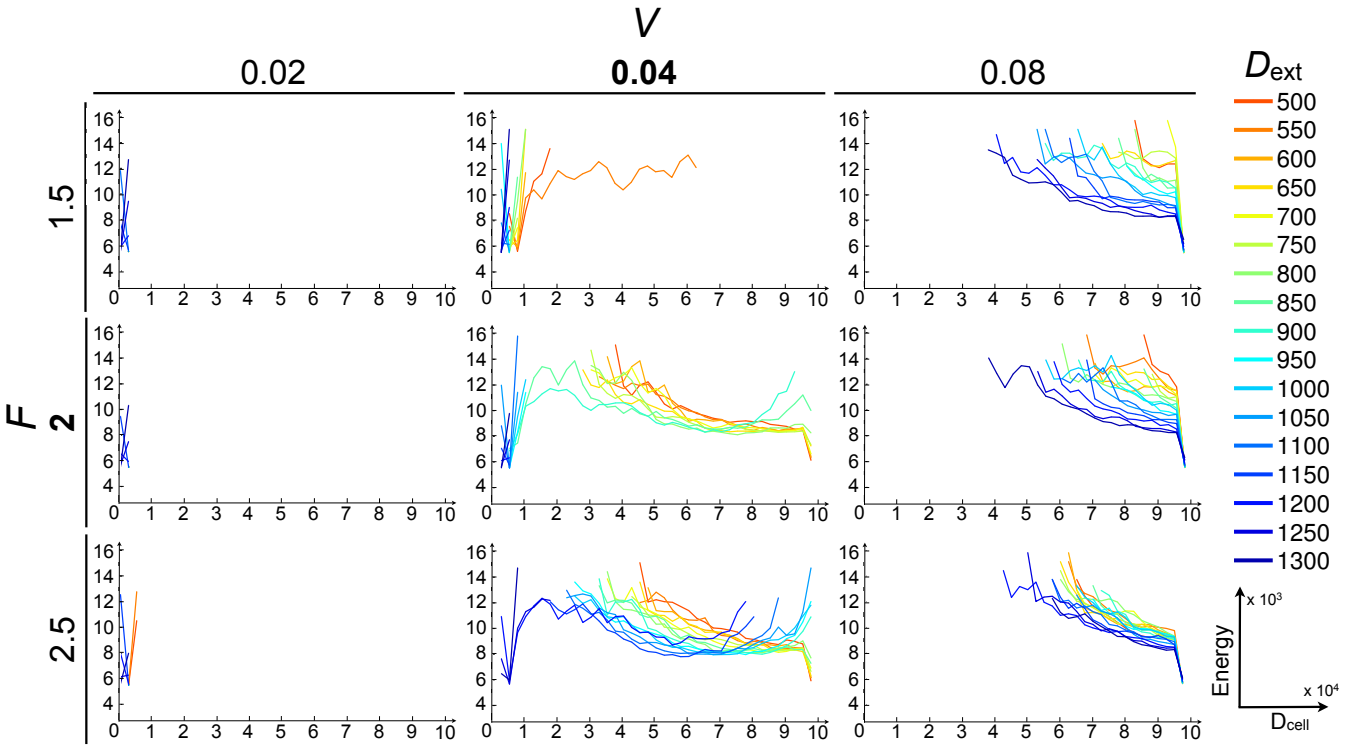

Figure 6. Free energy landscapes of the EC in the presence of constant D_{ext}, ranging from 550 (red) to 1300 (dark blue), as a function of V and F. Energy on the y-axis is calculated as $E = -log[p(D_{cell})]$. Bold V/F values (middle panel) mark the control (biologically calibrated) case.

by choosing 2250 as the threshold of transition from Fig. 4d, and measured the length of uninterrupted residence times in each state. Their distribution as a function of D_{ext} is shown in Fig. 5. As expected, an increase in D_{ext} leads to the appearance of long residence in the inhibited state. In the D_{ext} range of 700 – 1040, the EC is not easily stuck in either state, and often performs rapid back-and forth jumps across the barrier. These rapid jumps are most like in the middle of this D_{ext} window, where long residence in both active and inhibited states are equally likely.

Energy Landscapes

In addition to residence times, long simulations under constant D_{ext} also allow us to map the "free energy landscape" of the EC in different conditions. To this end, we binned the D_{cell} range (B = 250), measured the number of non-consecutive time-steps the EC has D_{cell} in each bin [$n(D_{cell})$] and calculated the probability distribution

$$p(D_{cell}) = n(D_{cell}) / (B \cdot n_{max})$$

for each target D_{ext} (n_{max} is the total number of time-steps). The free energy of the EC is then proportional to $-log(p)$. As expected, for intermediate D_{ext} values the energy landscape has two robust local minima (Fig. 6, control case: F = 2; V = 0.04). We tested the effect of altering active perception on the energy landscape. We find that a double-well energy landscape (and bistability) requires a balance between F and V. For example, altering V has a profound effect within the analyzed range of $D_{ext} \in [550, 1300]$ (values that bracket the range of bistability for the control case). Weak / strong V completely destabilizes the active/inhibited state for this D_{ext} range, and renders the EC monostable. On the other hand F can only destabilize the active state when it is weak. Strong F results in a deeper potential well for the active state, without destabilizing the inhibited valley.

Collective patterning is temporally determined by active perception

So far we have focused on a single EC between fixed neighbors. However, if we have two ECs armed with active perception, they can form individual bistable switches, while *D-N* lateral inhibition between them guarantees that only one of them can exist in an active state at one time. This circuit design thus guarantees that two neighboring ECs form a higher-level bistable switch. In the setting of a multi-cell collective and in the presence of the input gradient they readily generate the S&P pattern (Fig 7a). In the single cell case, when F is reduced, or V is altered, the active perception and therefore bistability of the cells is weakened. This slows down the collective allocation of heterogeneous migratory phenotype (Fig 7b,c).

Discussion

This study represents a first step towards a new understanding of how coordinated movement decisions in heterogeneous collectives can be made efficient and robust. This paper presents the establishment of a new testbed, the APB model, and validation that the central hypothesis "active perception generates bistability" can be accepted. Hence active perception and the *move and decide* perspective provide a novel explanation as to how heterogeneous states are so rapidly and robustly assigned in the collective morphogenesis of blood vessel growth. The bistability of single ECs faced with the intermediate levels of inhibition, typical of unpatterned phases, guarantees that state changes occur abruptly (rapid). Moreover, bistability confers short-term memory to EC states in the face of small fluctuations (robustness). The sensitivity of angiogenesis to VEGF gradient and concentration changes in disease can now be viewed as an active perception defect. Overall, this study provides novel biological predictions, to be tested *in vitro*. How full cell movement, collective rearrangement and other signaling pathways feed back and interplay with active perception and collective bistability remains to be investigated in futures studies.

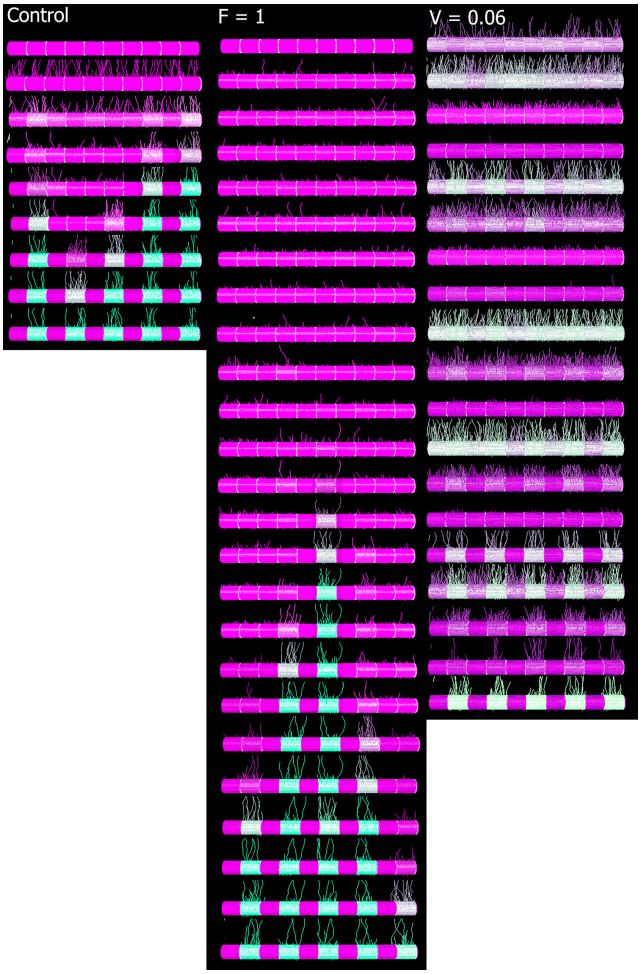

Figure 7. Time-space plots showing simulations with ten cells, periodic boundary conditions and lateral inhibition coupling. Frames every 100 time-steps shown vertically (Dll4 level high-low shown green-purple). It takes approx. 700t to reach the S&P pattern in normal conditions (Control, left panel). Halving the probability of filopodia (F = 1, middle panel) slows down the collective patterning by over three times Control. Increasing the input signal (V = 0.06, right panel) also slows down collective patterning, but this time due to the cell's synchronously oscillating whilst deciding, as the excessive input causes delayed excessive inhibition.

The reason for the positional interchanges during vascular morphogenesis is not yet known, though the dynamic and plastic nature of the cell phenotypes likely contributes to the adaptive capability of the collective network. This suggests that constant re-allocation of agent behaviors in heterogeneous collective systems via dynamic coordination, such as the active-perception-lateral-inhibition mechanism here, may also confer greater adaptability and robustness to collective robotics. Examples include systems where group plasticity facilitates role coordination, temporary scaffolds, and collective construction (Petersen et al 2011). Thus further study could also reveal important insights for morphogenic engineering principles.

Acknowledgments. KB is funded by BIDMC. ERR is funded by BIDMC and grant HL077348-03 from the NIH. KIH is funded by the Brandeis University Department of Computer Science, and thanks Jordan Pollack for support.

References

Aird, W. C. "Spatial and temporal dynamics of the endothelium. (2005). *Journal of Thrombosis and Haemostasis* 3(7):1392-1406.

Angeli D., Ferrell J. E., Sontag E. D. (2004). Detection of multistability, bifurcations, and hysteresis in a large class of biological positive-feedback systems. *Proceedings of the National Academy of Sciences, U.S.A,* 101:1822-1827.

Beer, R. D. (2000). Dynamical approaches to cognitive science. *Trends in cognitive sciences*, *4*(3), 91-99.

Bentley, K., Gerhardt, H., & Bates, P. A. (2008). Agent-based simulation of notch-mediated tip cell selection in angiogenic sprout initialization. *Journal of Theoretical Biology*, *250*(1), 25-36.

Bentley, K., Mariggi, G., Gerhardt, H., & Bates, P. A. (2009). Tipping the balance: robustness of tip cell selection, migration and fusion in angiogenesis. *PLoS computational biology*, *5*(10), e1000549

Bentley, K., Franco, C. A., Philippides, A., Blanco, R., Dierkes, M., Gebala, V., ... & Gerhardt, H. (2014a). The role of differential VE-cadherin dynamics in cell rearrangement during angiogenesis. *Nature cell biology,* 16*:*309-321.

Bentley, K. Philippides, A. and E. Ravasz Regan. (2014b) Do Endothelial Cells Dream of Eclectic Shape? *Dev. Cell.* In Press.

Cherry J. L., Adler F.R. (2000). How to make a biological switch. *J Theor Biology,* 203:117–133.

Collier, J. R., Monk, N. A., Maini, P. K., & Lewis, J. H. (1996). Pattern formation by lateral inhibition with feedback: a mathematical model of delta-notch intercellular signaling. *Journal of Theoretical Biology*, *183*(4), 429-446

Dewey, J. (1896) The Reflex Arc Concept in Psychology. *Psychological Review*, *3*, 357-370.

Doursat, R., Sayama, H., & Michel, O. (2012). *Morphogenetic Engineering: Toward Programmable Complex Systems*. Springer.

Ferrell J. E. (2002) Self-perpetuating states in signal transduction: positive feedback, double-negative feedback and bistability. *Current Opinions in Cell Biology*, 14:140 –148.

Gardner T. S., Cantor C. R., Collins J. J. (2000). Construction of a genetic toggle switch in Escherichia coli. *Nature*, 403:339 –342.

Geudens, I., & Gerhardt, H. (2011). Coordinating cell behaviour during blood vessel formation. *Development*, *138*(21), 4569-4583.

Hellström, M., Phng, L. K., Hofmann, J. J., Wallgard, E., Coultas, L., Lindblom, P., ... & Betsholtz, C. (2007). Dll4 signalling through Notch1 regulates formation of tip cells during angiogenesis. *Nature*, *445*(7129), 776-780.

Jakobsson, L., Bentley, K., & Gerhardt, H. (2009). VEGFRs and Notch: a dynamic collaboration in vascular patterning. *Biochemical Society Transactions*, *37*(6), 1233.

Jakobsson, L., Franco, C. A., Bentley, K., Collins, R. T., Ponsioen, B., Aspalter, I. M., ... & Gerhardt, H. (2010). Endothelial cells dynamically compete for the tip cell position during angiogenic sprouting. *Nature cell biology*, *12*(10), 943-953.

Petersen, K., Nagpal, R., & Werfel, J. (2011). Termes: An autonomous robotic system for three-dimensional collective construction. *Proc. Robotics: Science & Systems VII*.

Pfeifer, R.a.C.S. (1997). Sensory-Motor Coordination: The Metaphor and Beyond. Robotics and Autonomous Systems *20*, 157--178.

Piaget, J. (1967). A child's conception of Space (Norton, New York).

Van Duijn, Marc, Fred Keijzer, and Daan Franken (2006). "Principles of minimal cognition: Casting cognition as sensorimotor coordination." *Adaptive Behavior* 14(2): 157-170.